Solution-Engineered Palladium Nanoparticles: Model for Health Effect Studies of Automotive Particulate Pollution

Kai E. Wilkinson,[†] Lena Palmberg,[‡] Erika Witasp,[‡] Maciej Kupczyk,[‡,§] Neus Feliu,[‡] Per Gerde,[⊥,‡] Gulaim A. Seisenbaeva,[†] Bengt Fadeel,[‡] Sven-Erik Dahlén,[‡,§] and Vadim G. Kessler[†,*]

[†]Department of Chemistry, Biocenter, Swedish University of Agricultural Sciences (SLU), Box 7015, SE-75007, Uppsala, Sweden, [‡]Institute of Environmental Medicine, and [§]Centre for Allergy Research, Karolinska Institutet, SE-17177 Stockholm, Sweden, and [⊥]Inhalation Sciences Sweden AB, Karolinska Institutet, Science Park, SE-171 77 Stockholm, Sweden

ABSTRACT Palladium (Pd) nanoparticles are recognized as components of airborne automotive pollution produced by abrasion of catalyst materials in the car exhaust system. Here we produced dispersions of hydrophilic spherical Pd nanoparticles (Pd-NP) of uniform shape and size (10.4 ± 2.7 nm) in one step by Bradley's reaction (solvothermal decomposition in an alcohol or ketone solvent) as a model particle for experimental studies of the Pd particles in air pollution. The same approach provided mixtures of Pd-NP and nanoparticles of non-redox-active metal oxides, such as Al_2O_3. Particle aggregation in applied media was studied by DLS and nanoparticle tracking analysis. The putative health effects of the produced Pd nanoparticles and nanocomposite mixtures were evaluated *in vitro*, using human primary bronchial epithelial cells (PBEC) and a human alveolar carcinoma cell line (A549). Viability of these cells was tracked by vital dye exclusion, and apoptosis was also assessed. In addition, we monitored the release of IL-8 and PGE_2 in response to noncytotoxic doses of the nanoparticles. Our studies demonstrate cellular uptake of Pd nanoparticles only in PBEC, as determined by TEM, with pronounced and dose-dependent effects on cellular secretion of soluble biomarkers in both cell types and a decreased responsiveness of human epithelial cells to the pro-inflammatory cytokine TNF-α. When cells were incubated with higher doses of the Pd nanoparticles, apoptosis induction and caspase activation were apparent in PBEC but not in A549 cells. These studies demonstrate the feasibility of using engineered Pd nanoparticles to assess the health effects of airborne automotive pollution.

KEYWORDS: palladium · nanoparticles · cytotoxicity · air pollution · health effects · catalytic converter

The worldwide increase in automobile usage is directly correlated with the population increase, and thus more vehicular activity is present in densely populated areas.[1−3] This has been shown to have implications on the health of individuals residing or working in polluted areas,[4] as it is well known that inhalation of polluted air, more specifically the particulate matter (PM) suspended in air, can cause detrimental health effects including cardiovascular and respiratory disease.[5] For individuals with pre-existing conditions such as asthma and chronic obstructive pulmonary disease (COPD) the effects can be more severe, such as hospitalization or in the worst case premature death.[6]

The platinum group metals (PGMs) (Ru, Os, Rh, Ir, Pd, and Pt) are all present in very low concentrations in the earth's upper crust and do not naturally occur in any appreciable airborne amounts.[7,8] Higher concentrations of PGMs occur in certain geographic locations, enabling their extraction and use on an industrial scale. The main use of these metals is in automobile catalytic converters, where over 60% of the procured metals are used.[9] Almost all localized prevalence of PGMs can be derived from automobile exhaust emissions related to the abrasion of the catalytic converter and from industrial smelter activity.[10−12] Catalytic converters are constructed by depositing approximately 0.2 wt % of PGMs on a honeycomb-cordierite substrate ($MgO \cdot Al_2O_3 \cdot 2.5SiO_2$) covered by a washcoat of cordierite and γ-Al_2O_3.[13,14] The high surface area of the honeycomb structure and that of the porous cordierite enables the exhaust gas to react with the PGMs dispersed in the substrate material. The common constellation of PGMs in catalytic converters is that Pt and Rh are used for reduction reactions, while Pd and Pt are used for oxidation reactions, although differences in PGM composition occur as a consequence of countries having differing legislation and environmental requirements.[14]

Inhalation is the primary route of exposure to PM. Whether the inhalable PM is of micro- or nanosize (10−0.1 μm and <100 nm, respectively), evidence shows that the

* Address correspondence to vadim.kessler@slu.se.

Received for review November 30, 2010 and accepted June 8, 2011.

Published online June 08, 2011
10.1021/nn1032664

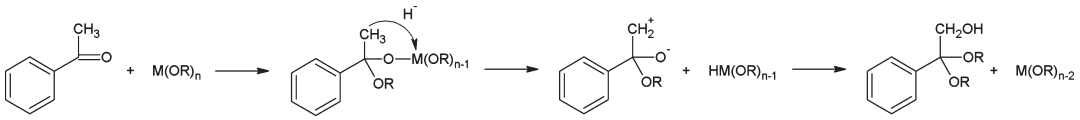

Scheme 1. Proposed reaction pathway for Bradley's reaction of nanoparticle synthesis in acetophenone.

deposition of particles is similar and occurs on the same time scale.[15] In contrast, there are major differences in how particles are absorbed and how they interact with the bodily environment once taken up into tissue and their clearance out of the organism: microparticles are generally taken up in the lungs and retained there, whereas nanoparticles (NPs) have the possibility of crossing membranes, by active uptake or diffusion, and being distributed throughout the body in various organs, lymphatic and blood circulation, *etc*.[16] The size of the particle itself does not necessarily govern a particle's toxicity, but the inherent surface properties do,[17] and NPs therefore exhibit gram-for-gram a proportionately higher surface area and thus a stronger reactivity than microsized particles. It is not well known where the actual toxicity stems from: whether it is soluble species released from the particles or the extended surface area of NPs causing the creation of reactive oxygen species.

While catalytic converters are effective at converting gaseous emissions into less harmful forms, they do not wholly alleviate the emission of particulate pollution. Furthermore automobiles with diesel engines can be fitted with particle filters, but these do not stop the emission of incombustible nanoparticulates.[18] The way in which PGMs are impregnated into the cordierite substrate produces a nanoparticulate form of PGMs. These are emitted in time through abrasion and wear in the catalyst in detectable amounts as an aerosol.[19] Although the weight distribution of PGM emission is largest in the micrometer range, it is not inconceivable that particulate agglomeration of smaller species occurs upon exiting the exhaust system. PGMs are considered toxic, especially in their soluble form, and have been shown to be bioaccessible when ingested.[20−22] A problem arises when complexation in the environment through natural ligands occurs and the ions are produced. These may further react to form halogen compounds, which are considered highly toxic and allergenic.[23] While agglomeration of the NPs will occur in air, their inherent chemistry when in a bodily environment is dictated by their high surface area, and the toxicity of these nanoparticulates should be evaluated more thoroughly.[24−29]

Risk assessment of the health impact of the kind of particles that are being emitted from catalytic converters is important, but the use of existing catalytic material from converters to make NPs could be arduous and it is difficult to obtain a strict size distribution. An attractive alternative for production of the model nanoparticle fraction is solution synthesis. Traditional approaches to palladium colloids utilize either aqueous or nonaqueous reduction of palladium salts. In the aqueous route it is most commonly chloride or acetate that is reacted with sodium hydroboride, $NaBH_4$, as reducing agent.[30] This approach has to be ruled out for the use in bioactivity studies, as the produced byproduct, the boric acid, is a well-recognized bactericide. Another common approach is exploiting the thermal decomposition of palladium salts with organic anions such as acetate or acetylacetonate in xylene as solvent, often using oleic acid as surfactant. This approach results in hydrophobic samples, impossible to dilute with or disperse in an aqueous medium.[31] Other novel methods involve the use of tobacco mosaic virus, ultrasonication (sonochemical synthesis), and peptides in synthesizing Pd-NPs.[26−28] For a brief summary of other synthesis methods, see Li *et al*.[29] Better analogues of the particles in question can be synthesized by utilizing Bradley's reaction,[32−34] a solvothermal process based on ether elimination in an alcohol or carbonyl compound medium (see Scheme 1).[35] The reaction does not use any harmful or persistent chemicals and can be carried out under relatively mild conditions, making it a very versatile tool for producing NPs. Moreover, the precipitate is hydrophilic and thus easily redispersed in aqueous solutions, making it amenable to *in vitro* studies.

Most studies with particulate air pollutants in cell cultures have been made with cells under submerged conditions in culture flasks. The dose is characterized as an average particle concentration per volume of medium. While the drawback is a rather nonphysiological exposure condition with particles interacting with a relatively large volume of medium before potentially interacting with the cells, the advantage is a relative ease of use and a large body of reference literature. A more realistic scenario is achieved during aerosol exposures of cells cultured under so-called air-lifted conditions in membrane inserts.[36] The deposited particles will be interacting with only a small volume of extracellular liquid before interaction with the target cells may occur. Toxic solutes from the particles will be less diluted, and particles will have increased opportunity to interact with the cells. There are some indications that typical air pollutants are more potent during exposures under air-lifted conditions.[36] The achieved doses are then quite often characterized on a surface basis. The advantage of greater realism is counterbalanced by a much greater technical difficulty and a much sparser body of reference data. Therefore in the current study we chose to characterize the novel

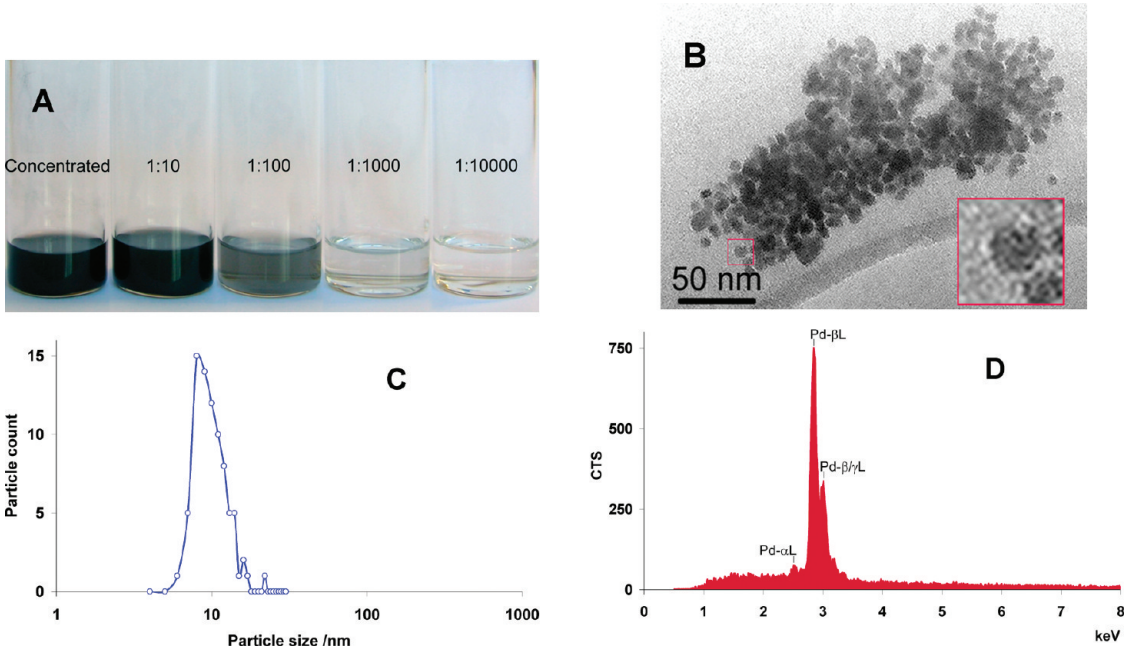

Figure 1. Characterization of solution-engineered palladium nanoparticles (Pd-NPs). (a) Dispersion of Pd-NPs in ethanol, (b) TEM image of Pd-NPs on a copper grid (inset box width approximately 16 nm, showing single 11 nm wide palladium particle), (c) size distribution of as-synthesized Pd-NPs determined from TEM images, (d) representative EDS spectrum of Pd-NPs (the L lines of Pd were mainly observed in the 0.5−8 keV interval).

materials using well-controlled, submerged exposure conditions.

The PGM emitted the most (on a mass basis) is Pd, and we present in this paper a method of synthesizing Pd-NP analogues using wet chemistry and perform toxicity studies for analogues of emitted metallic Pd-NPs and Pd−Al-oxide NP-nanocomposites using two different and relevant cell types representative of the human lung epithelium including primary bronchial epithelial cells.

RESULTS AND DISCUSSION

In the present study, metallic Pd-NPs were synthesized by refluxing palladium acetylacetonate, $Pd(acac)_2$, solution in acetophenone at 202 °C (bp of the solvent). The solvent in the resulting dispersion of produced Pd-NPs was then exchanged for ethanol (99.5%) before proceeding to testing of particles on cells (see Figure 1a). The size, shape, and crystallinity of the precipitate were characterized using transmission electron microscopy (TEM) and powder X-ray diffraction (XRD). A sample of a nanocomposite of Pd combined with Al_2O_3 (Al:Pd = 10:1) was synthesized by the same approach using aluminum isopropoxide, $Al(O^iPr)_3$, as additional precursor and characterized, to further simulate emitted Pd particles containing a semblance of the Al_2O_3 honeycomb structure still attached to the Pd metal. The morphology of the obtained Pd-NPs (see Figure 1b) is clearly defined as spherical and uniform in shape. The XRD revealed the sample to be mostly crystalline, containing the cubic phase of Pd metal (*Fm*3) along with an admixture of an amorphous phase of palladium metal (see Supplementary Figure S1). The size distribution is based on 80 measured particles, from which a mean size and standard deviation can be derived: 10.4 ± 2.7 nm (Figure.1c). SEM-EDS analysis (Figure1d) confirmed the presence of pure Pd-NPs (for nanocomposite material see Supplementary Figure S2). In the $Pd-Al_2O_3$ sample one can easily, due to electron-density-related contrast, see slightly larger and darker Pd particles randomly distributed among smaller (average size about 2−3 nm) and lighter particles of Al_2O_3 (Supplementary Figure S3).

Characterization of the particles was performed in water and the cell culture media used for culturing A549 and PBEC cells, respectively, using dynamic light scattering (DLS) and nanoparticle tracking analysis (NTA, NanoSight) techniques. Both techniques provide size mode distribution of particles and aggregates in the measured fluid but do so in slightly different ways. In DLS the Brownian motion of particles is measured by detection of light scattering of individual particles, being preset to detect scattering from a specific index of refraction (in this case 4.1 for Pd). The NTA method, on the other hand, uses laser reflections from individual particles and maps their Brownian motion in real time by CCD camera (the motion is dependent on the size of the particles, density of material, and viscosity of the solvent), producing a statistically reliable direct observation of size distribution.[37] The results for these experiments can be seen in Figure 2. In water and PBEC cell culture medium the particles seem to organize into aggregates with size mode of approximately 100 nm. The observed *z*-potential is close to zero in water with a

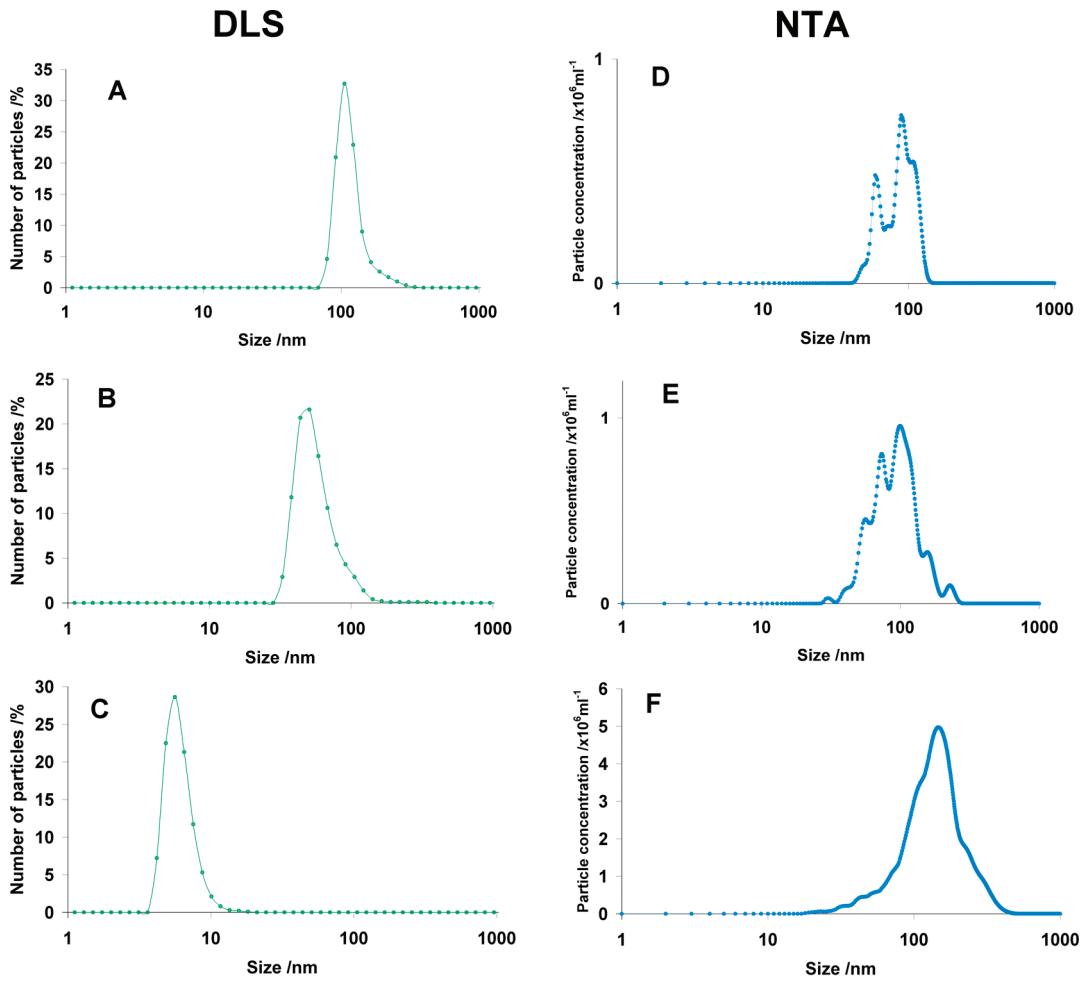

Figure 2. Comparison of particle aggregation modes in filtered (0.45 μm) ultrapure water (Milli-Q) and PBEC and A549 growth media as measured by dynamic light scattering (Malvern Z-Sizer DLS) (A, B, and C, respectively) and nanoparticle tracking analysis (NTA, Nanosight LM10 HSB) (D, E, and F, reapectively).

broad and unstable in time distribution of particle charges, as it is usually observed for nanoparticles prepared in organic media and transferred to water without surface modification.[38] The potentials in PBEC and A549 culture media are negative, −15.3 and −12.8 mV, respectively, reflecting the adsorption of anions from solution. In A549 cell culture medium the aggregation can be seen in the NanoSight sample (the observed particles are apparently protein micelles present in the cell medium used in this case; the particles smaller than approximately 15 nm are not visible in this technique because of low reflecting ability), but interestingly is absent in the DLS sample, being replaced by individual particles (*cf.* Figure 1c). The protein micelles are not displayed in DLS because their signal is removed, applying the cut-offs relevant for Pd particles. Stabilization of single particles visible in DLS results has a plausible explanation in the fact that the particles interact somehow with, for example, albumin and are stabilized in solution as individual particles. This could also explain results from cell uptake studies using A549 cells (see below). Whether the particles are stabilized by proteins and, if so, by what proteins certainly deserves further study and will not be speculated upon in the present paper.

Vallhov and co-workers determined the importance of an endotoxin-free environment for the production of nanoparticles for biological assessment.[39] We assessed whether the Pd-NPs were endotoxin-free using the conventional LAL test, as described in Methods. The results revealed that the concentration of endotoxin found in various Pd-NP batches was below the critical limit mandated by the U.S. Food and Drug Administration for acceptance for the chromogenic LAL assays (Supplementary Figure S4).[40] The level of LPS is thus lower than the amount of LPS required to stimulate cytokine release in A549 cells or PBEC.[41,42]

In order to assess the possible toxicity of Pd-NPs, cellular studies were performed using human primary bronchial epithelial cells (PBEC) as a model for the epithelial cells in the upper respiratory tract, which most commonly come in contact with inhaled particulates. Also, A549 immortalized alveolar basal human epithelial cells were used to simulate the lower respiratory tract,

where most of the smaller inhalable particles are usually deposited. Moreover, the use of primary cells is important when assessing possible health effects of engineered nanomaterials, as transformed cell lines and primary cells may react differently, even when the cells are derived from the same tissue.[43] Using vital dye exclusion as a marker of cytotoxicity, we demonstrated that Pd-NPs do not affect cell viability of PBEC or A549 cells at doses up to 10 μg/mL of Pd-NP (Supplementary Table 1). However, Pd-NPs affect cell viability at higher doses. Of note, PBEC were markedly more affected by Pd-NPs than A549 cells (Figure 3). Cell death was further evaluated using propidium iodide (PI) staining to detect DNA fragmentation, a marker of apoptosis. As seen in Figure 4a, apoptosis was triggered in a dose-dependent manner in PBEC cells, but not in A549 cells. The protein kinase C inhibitor staurosporine (STS) was used as a positive control in both cell lines. To further dissect the mechanism of cell death, we tested whether Pd-NPs activated caspases (cytsteine-dependent, aspartate-specific proteases). We observed that 25 μg/mL Pd-NPs induced caspase-3-like enzyme activity in PBEC cells, as evidenced using the DEVD-AMC assay (Figure 4b). No caspase activation was seen in A549 cells (data not shown). Moreover, the cleavage of pro-caspase-3 to active caspase-3 in PBEC cells, but not

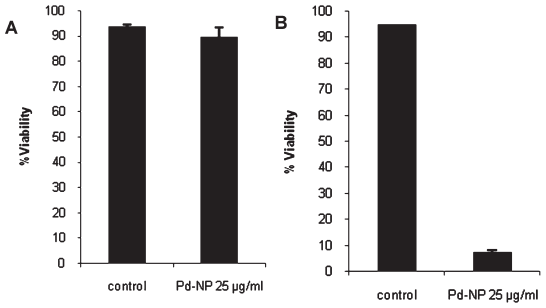

Figure 3. Effect of Pd-NPs on viability of human lung epithelial cells. A549 cells (A) or PBEC (B) were exposed to 25 μg/mL Pd-NPs for 24 h, and the percentage of viable cells was assessed by Trypan blue exclusion. Data shown are mean values of three independent experiments (A549) (n = 3) or of two different human donors (PBEC) (n = 2) ± SEM.

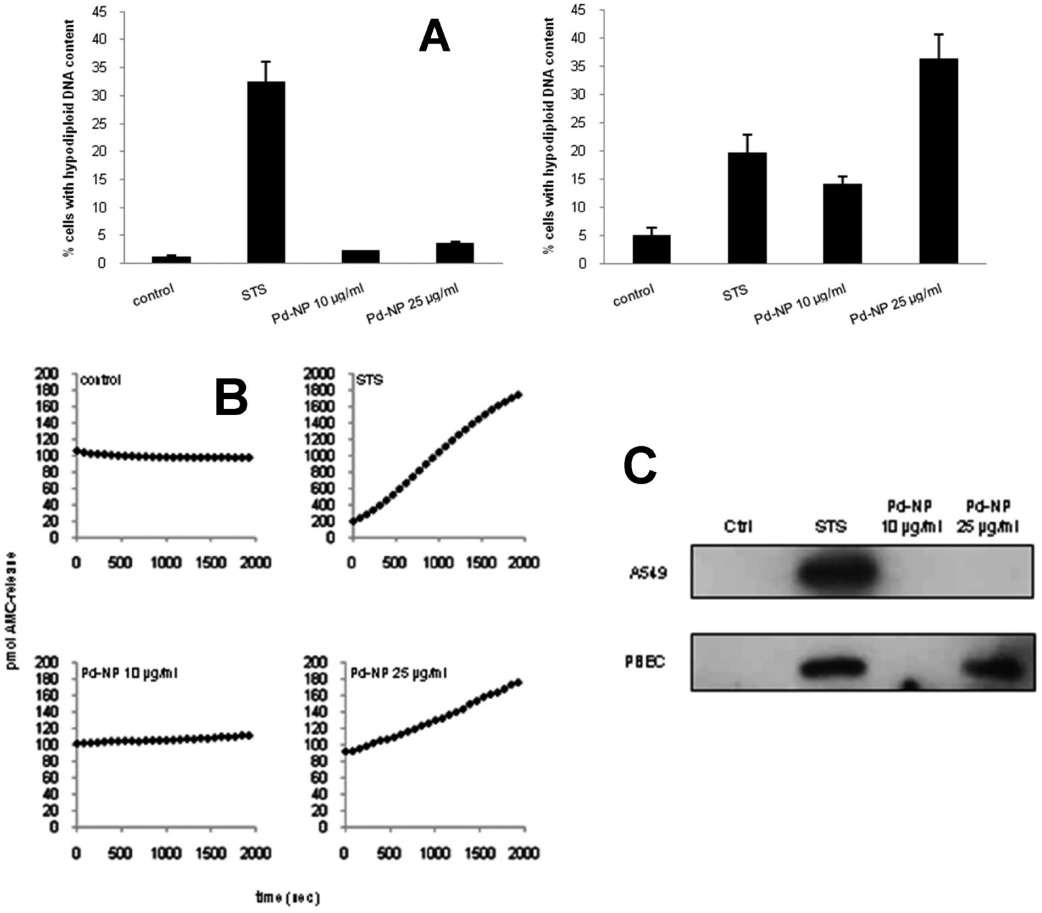

Figure 4. Induction of apoptosis by Pd-NPs in PBEC. Cells were exposed to 10 or 25 μg/mL Pd-NPs for 24 h and thereafter assessed for characteristic features of apoptosis. Cells treated with staurosporine (STS) were included as a positive control for apoptosis. (A) PI staining of A549 (left graph) and PBEC (right graph) revealed hypodiploid DNA content in cells upon treatment with Pd-NPs. Data shown are mean values ± SEM (n = 3). (B) Real-time measurements of AMC release (indicative of caspase-3-like enzyme activity) in cell lysates from PBEC. Note the different scale on the y-axis of STS due to very high levels of enzyme activity. Results are representative of several independent experiments. (C) Processing of pro-caspase-3 (32 kDa) to active caspase-3 (17 kDa) in PBEC was analyzed by Western blotting using a polyclonal antibody specific for the active cleavage fragment of caspase-3. STS-treated cells were included as a positive control.

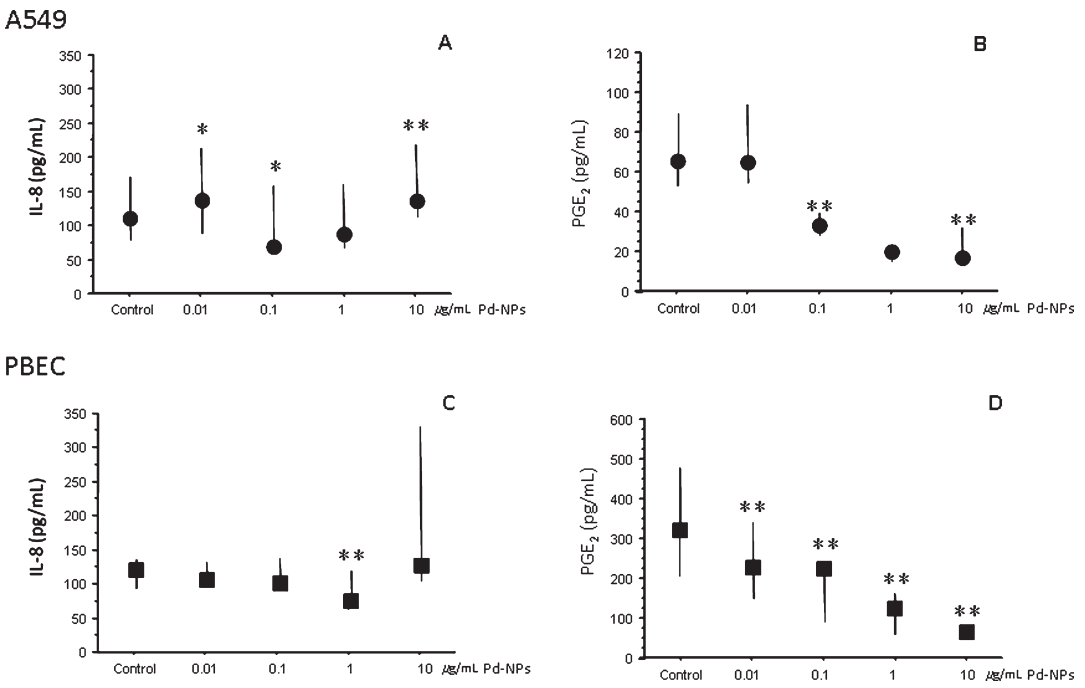

Figure 5. Effect of Pd-NPs on human lung epithelial cells. Pd-NPs were added at the indicated concentrations to A549 (a and b) and PBEC (c and d), and the release of IL-8 (a and c) or PGE_2 (b and d) was determined. Data are presented as median and interquartile range. Comparisons were made using Wilcoxon signed rank test. A *p*-value less than 0.05 was considered significant. *$p < 0.05$ and **$p < 0.01$ compared to the control.

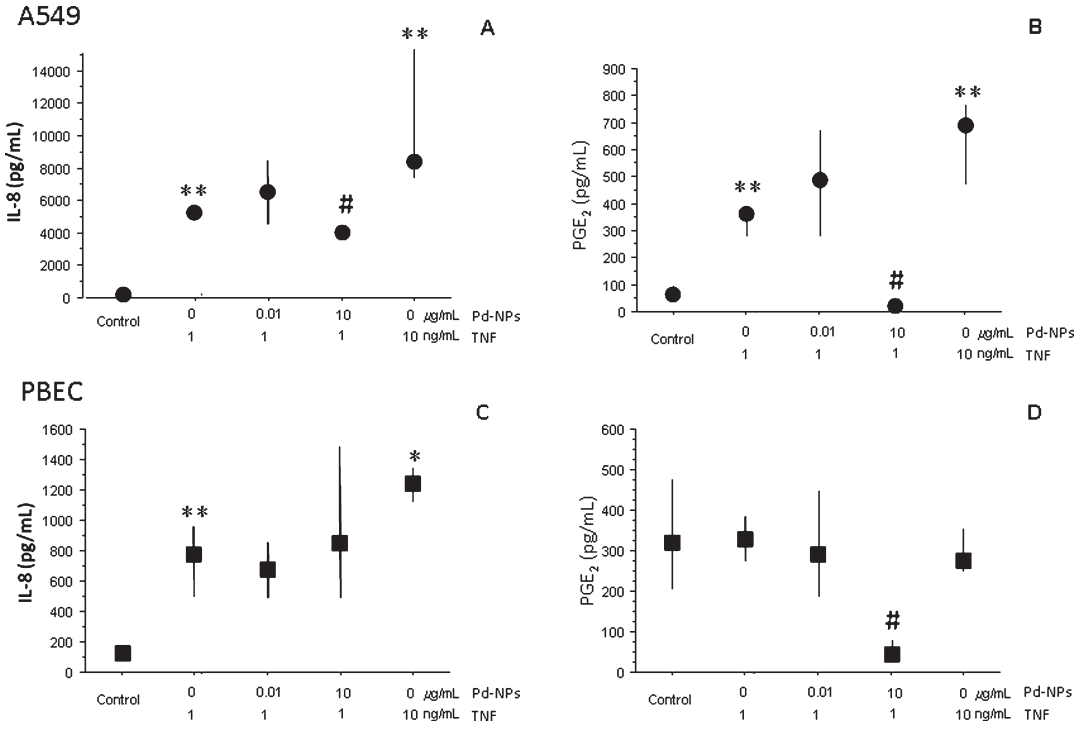

Figure 6. Effect of Pd-NPs on TNF-α-induced stimulation of lung epithelial cells. The effect of TNF-α (1 ng/mL) alone or in combination with Pd-NP (0.01 and 10 μg/mL) in A549 (a and b) and PBEC (c and d) and the release of IL-8 (a and c) or PGE_2 (b and d) was determined. As a positive control, TNF-α at a concentration of 10 ng/mL was used. Data are presented as median and interquartile range. Comparisons were made using Wilcoxon signed rank test. A *p*-value less than 0.05 was considered significant. *$p < 0.05$ and **$p < 0.01$ compared to the control; $^{\#}p < 0.05$, the combination of Pd-NP and TNF-α compared to TNF-α alone at the same concentration.

in A549 cells, was confirmed by immunoblotting of the active fragment of caspase-3 (Figure 4c).

The cytotoxicity of certain nanoparticles can be explained by their propensity to induce oxidative stress.[44]

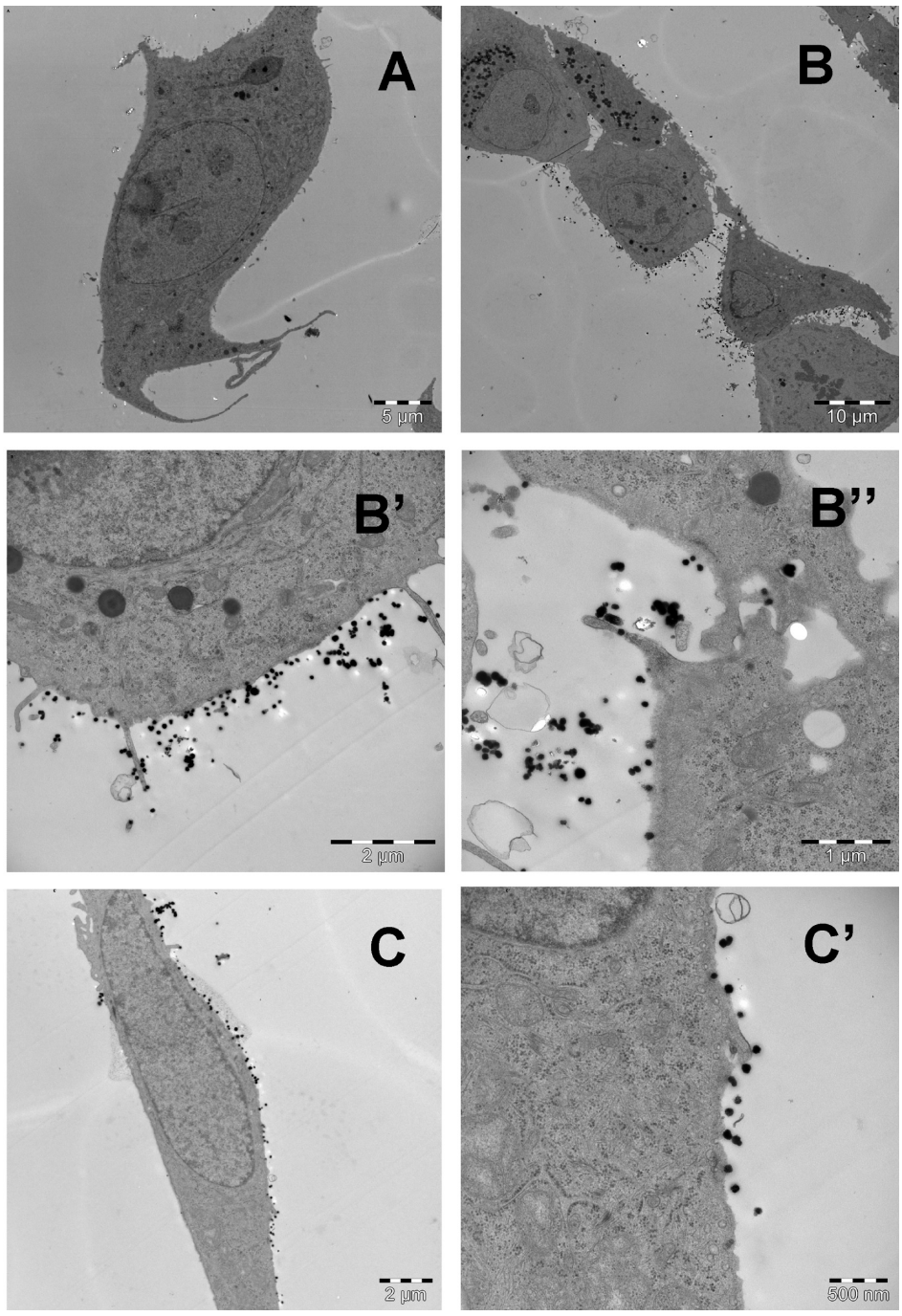

Figure 7. Internalization studies of Pd-NPs by A549 cells. Micrographs of A549 cells (A). A549 cells exposed to 10 μg/mL of Pd-NPs for 2 h (B, B″ and C, C′). B′, B″, and C′ are high magnification views from B and C, respectively. Scale bars: A: 5 μm; B: 10 μm; C: 2 μm; B′: 2 μm; B″, C′: 500 nm.

However, the Pd-NPs utilized in the current study elicited only modest levels of reactive oxygen species production in cells (Supplementary Figure S5). Kim *et al.*,[27] Kajita *et al.*,[47] and Hikosaka *et al.*[48] have shown that Pt nanoparticles can function as antioxidants in that they alleviate induced oxidative stress in nematodes. They have even postulated that this effect should occur also in humans and recommended Pt-NPs for medical use. Pd has very similar chemical traits to those of Pt, so it is plausible to suggest that they may be acting in this case in a similar capacity.

For assessment of the secretion of soluble biomarkers, we utilized doses up to 10 μg/mL for both cell types. The chemokine interleukin-8 (IL-8) is an important chemoattractant and activator or neutrophil and is produced by airway epithelial cells, neutrophils, and macrophages. Increased IL-8 levels have been shown in a number of inflammatory disorders including COPD and fibrotic lung diseases. Moreover, IL-8 secretion has been extensively investigated as an indicator of the inflammogenic potential of particles.[45] Prostaglandin

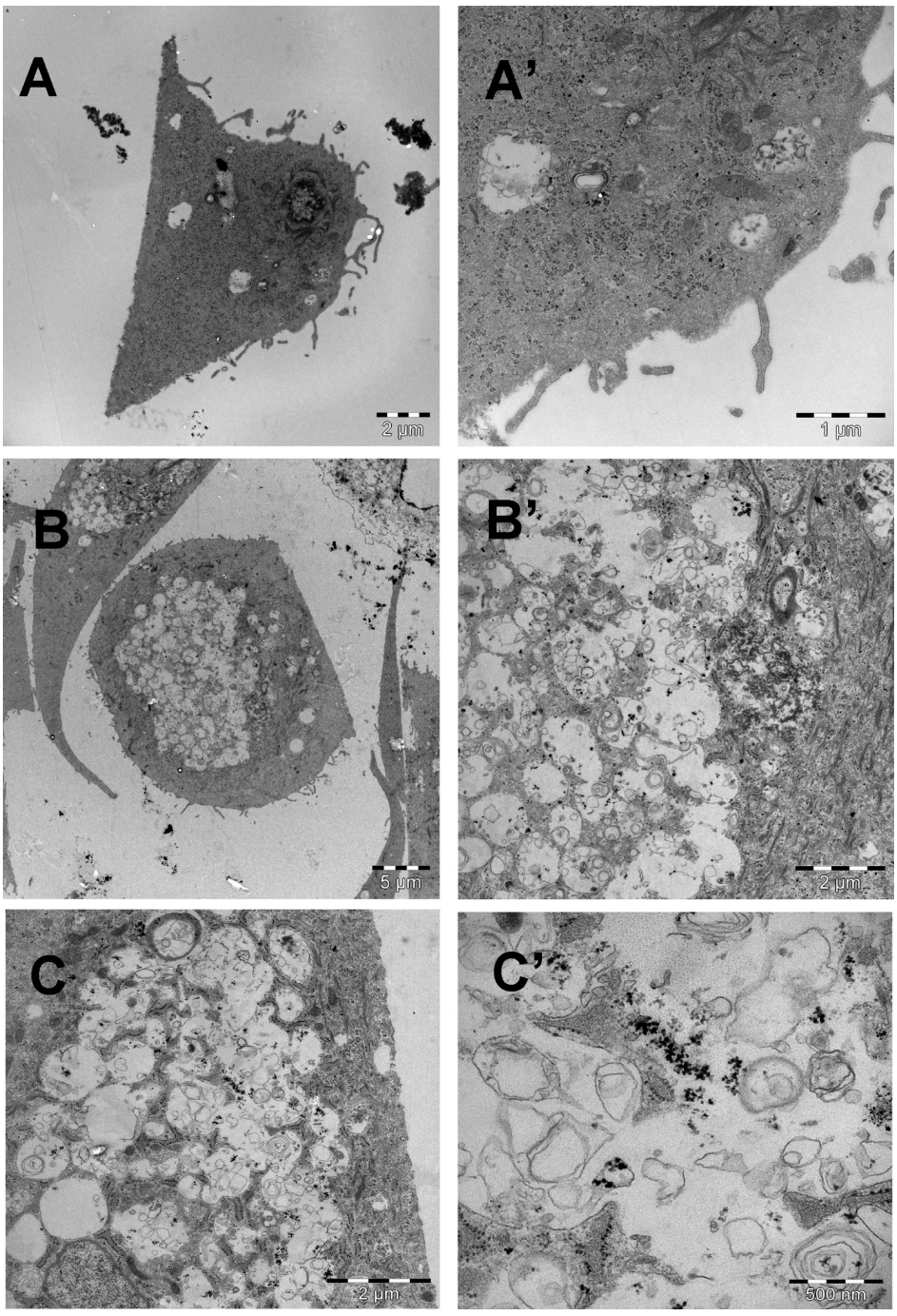

Figure 8. Internalization of Pd-NPs by PBEC. Micrographs of PBEC (A, A′) and PEBC exposed to 10 μg/mL of Pd-NPs for 2 h (B, B′ and C, C′). B′ and C′ are high magnification views from B and C, respectively. Scale bars: B: 5 μm; A, B′, C: 2 μm; A′: 1 μm; C′: 500 nm.

E_2 (PGE_2) is a primary product of arachidonic metabolism and is synthesized *via* the cyclooxygenase (COX) and prostaglandin synthase pathways. The important sources of PGE_2 in the airways include mast cells, dendritic cells, epithelial cells, and airway smooth muscle cells. PGE_2 has a number of biological actions, including vasodilation and both anti- and proinflammatory action.

As seen in Figure 5, the effect of Pd-NPs on the secretion of IL-8 by lung epithelial cells is distinctly nonlinear, with a concentration-dependent decrease in the lower concentration range and a slight tendency of increased levels at the highest concentration (Figure 5a,c). On the other hand, secretion of the lipid mediator PGE_2 exhibits a clear and concentration-dependent decrease in both cell types (Figure 5b,d). Notably, these effects are seen at a noncytotoxic concentration of Pd-NPs, indicating that these biomarkers serve as sensitive indicators of the biological effects of Pd-NPs. We also assessed the effect of Pd-NPs on tumor necrosis factor-α (TNF-α), a pro-inflammatory cytokine,

in an attempt to mimic an activated/pro-inflammatory state in our cell culture system. Our results show that 10 μg/mL Pd-NPs slightly increased the resistivity of the lung epithelial cells to TNF-α-induced IL-8 production (Figure 6 a,c) and PGE_2 production (Figure 6b,d). This effect is particularly clear for PGE_2. Of interest, in a very recent study, Boscolo *et al.*[46] reported that Pd salt inhibits cytokine release in primary human peripheral blood mononuclear cells, whereas Pd nanoparticles were found to exert immunomodulatory effects enhancing the release of IFN-gamma. The mechanism of cytokine regulation, however, was not disclosed.

We also assessed the effects of nanocomposites of Pd and non-redox-active metal oxides. The administration of Al_2O_3 alone to lung epithelial cells (A549) increased the release of IL-8 in a concentration-dependent manner. However, the addition of the Pd$-Al_2O_3$ nanocomposite material resulted in a decrease of IL-8 release (Supplementary Figure S6). This can be interpreted in terms of the well-known toxicity of Al^{3+} cations that are readily released on partial dissolution of the oxide nanoparticles in the cytosol. On the basis of these results, one may assume that the layer of sol$-$gel alumina covering the cordierite monoliths may be a reason for direct concern in relation to the health effects of exhausts from car catalysts. Further studies are warranted to address this issue.

Next, we studied cellular uptake of Pd-NPs using TEM. No uptake of particles could be observed within 2 h by A549 cells (Figure 7), but we observed nanoparticles immobilized on the cell surface. The uptake of Pd-NPs by PBEC, however, was more pronounced, and the majority of particles were found within membrane-bound vesicles (endosomes) inside the cells after 2 h (Figure 8a), suggestive of an active uptake mechanism.[49] No particles were detected in the nucleus. Differences in the composition of the cell medium and hence in the "corona" of proteins and other biomolecules could account for the differences in uptake that we observed between PBEC and A549 cells.[50] Notably, the A549 cells were cultured in cell medium containing 10% serum, while PBEC were cultured in serum-free medium but with the addition of epidermal growth factor and bovine pituitary extract. It is important to note that nanoparticles of metals and even metal oxides may not preserve their original active surface, as they are rapidly surface-functionalized with a "corona" of adsorbed biomolecules, which may guide their recognition and internalization by cells.[51,52] The observed differences between the two cell types may also be explained by the different origin of these cells: PBEC are derived from the upper respiratory tract, while A549 cells were used to simulate the lower respiratory tract. In addition, differences in terms of the propensity to internalize NPs may also be related to inherent differences between primary cells (PBEC) and transformed cells (A549) (for comparison, see ref 43). Other investigators have recently reported that cells from the respiratory tract actively ingest opsonized nanoparticles after 24 h exposure in cell culture.[53] The fact that cell uptake was monitored at 2 h could account for the apparent differences. Notwithstanding, our results demonstrate that PBEC are more prone to internalize Pd-NPs and are also more susceptible to cell death induction at higher doses of Pd-NPs when compared to A549 cells. The degree of cellular uptake is an important feature that may determine the toxic potential of particles and their biodistribution,[54] and further studies are warranted to investigate uptake mechanisms of Pd nanoparticles in PBEC.

CONCLUSIONS

We report on solution-engineered Pd and Pd$-Al_2O_3$ NPs as a model to assess the toxicity of automotive particulate pollution, using two different human lung epithelial cell types. Our studies show that these particles exert concentration-dependent cytotoxicity *in vitro*. Moreover, we provide evidence that Pd-NPs trigger caspase-dependent apoptosis in PBEC, but not in the A549 cell line, when cells are incubated at high doses of these particles. To the best of our knowledge, this is the first demonstration of Pd-NP-induced apoptosis.

Importantly, when administered at noncytotoxic doses, these particles display pronounced effects on the secretion of biomarkers by lung epithelial cells. It should be recognized that PGE_2 in human asthmatic airways has a protective anti-inflammatory role.[55,56] This means that the observed decrease in PGE_2 might indicate a toxic effect that potentially enhances airway inflammation. Furthermore, we report uptake of the particles by human epithelial cells. It is noted that the particle concentrations utilized herein remain relatively high and do not necessarily mirror those found in the environment. Nevertheless, the present studies provide a paradigm for the assessment of airborne particulate matter using engineered NPs as model particles. The introduction of such model particles in toxicological research may facilitate the comparison between studies performed in different laboratories and may also allow for the dissection of mechanisms of action of airborne particulate matter, in particular of PGMs derived from automobile exhaust emissions.

METHODS

Pd and Pd$-$Al Nanocomposite Particles. *Synthesis.* The Pd-NPs used in this study were synthesized using Bradley's reaction of solvothermal decomposition of Pd(II)-acetylacetonate (Pd[acac]). A 231 mg amount of 99% Pd(acac) (Aldrich) was deposited in a 50 mL flask under a nitrogen atmosphere (normal pressure), after which 20 mL of 99% reagent grade acetophenone (Aldrich) was added to the flask with a syringe through the rubber

stopper on the flask. The flask was vigorously shaken in order to dissolve the Pd(acac) and then connected to a water-cooled reflux column. The flask was heated and the contents were reflux-boiled for 4 h, causing a Pd-NP precipitate to form. The resulting particle suspension was transferred to a clean flask, with an additional 10 mL of acetophenone being added for the transfer. Solvent exchange was performed by coupling the flask to a vacuum-line and heating the flask slightly (while contents under vacuum pressure) and trapping the solvent vapor in a flask cooled by liquid nitrogen. Approximately 80−90% of the solvent was removed, and an equivalent amount of 99.5% analytical grade ethanol (Solveco) was added to the precipitate for resuspension. In total the solvent exchange was performed three times, and the final particle suspension solvent consisted of mainly ethanol. The Pd−Al nanocomposite NPs (10% Pd) were synthesized in the same manner as the Pd-NPs. In a nitrogen atmosphere, 186 mg of aluminum isopropoxide ($Al(O^iPr)_3$, Aldrich) was deposited into a 50 mL flask. Then 68 mg of Pd(acac) was deposited into a glass vial together with 10 mL of acetophenone. From the glass vial 4.65 mL of the liquid was transferred into the flask containing $Al(O^iPr)_3$, and 20 mL of acetophenone was added (10 mol % Pd). The reaction to produce the particle suspension under reflux was performed identically as for Pd-NP synthesis.

Characterization. Particle suspension from Pd, Pd−Al nanocomposite, and Al-NP was dried on carbon tape and analyzed using SEM energy dispersive spectroscopy (EDS) (Hitachi TM-1000 EDS) to ensure particle purity (EDS spectra for Pd−Al and Al-NP can be found in Supplementary Figure 2a and b). For TEM control of the particles, a drop of ethanol-diluted (1:10) particle suspension of Pd-NP and Pd−Al nanocomposite were deposited onto copper TEM grids and allowed to dry. The grids were then inserted into a Philips EM-STEM 400, and images were collected for the grids. The captured images were then scanned for Pd-NPs and Pd−Al NPs, and their diameter was measured using graphics editing software (Adobe Photoshop CS4 and GIMP2). In total 80 Pd and 560 Pd (Al-nanocomposite) individual particles were measured. The size distribution, size mean, and standard deviation of the mean could be determined on the basis of these measurements. The crystallinity of Pd-NPs was determined using X-ray powder diffraction. A sample was prepared by drying particles from solvent in an oven (approximately 90 °C) and grinding it into a fine powder. The resulting fine powder was collected in a 0.7 mm diameter glass capillary, which was then analyzed using a Bruker SMART Apex-II diffractometer utilizing Mo Kα radiation (0.71073 Å). The resulting patterns were analyzed using the EVA software package. The resulting diffraction pattern can be seen in Supplemental Figure 1S. Pd-NPs in ethanol were also diluted 1:10 in H_2O and A549 and PBEC cell culture media (see the cell culture sections below) and then filtered through 0.45 μm cellulose filters (pre-eluted using corresponding eluate). The filtered solutions were measured in a Malvern Z-Sizer DLS, giving a size distribution and *z*-potential surface charge of particles in solution. Also the same types of solutions were measured using a NanoSight LM10 HSB, and information pertaining to size mode of particles with respect to particle number was obtained.

Endotoxin Analysis. Lipopolysaccharide (LPS) concentrations were controlled by the end point chromogenic LAL test method (Limulus Amebocyte Lysate endochrome, Charles River Endosafe, Charleston, SC, USA).

Cell Culture. *Lung Carcinoma Epithelial Cell Line (A549).* The human lung carcinoma epithelial cell line A549 (American Type Culture Collection, Rockville, MD, USA) was cultured in 80 cm^2 plastic flasks (Nunc, Roskilde, Denmark) at a density of (1−2) × 10^6 in F-12 medium with 10% heat-inactivated fetal bovine serum and penicillin/streptomycin. The cultures were kept at 37 °C in a humidified atmosphere of 5% CO_2 in air, and medium was changed every second day. At confluence the cells were detached by exposure to trypsin/EDTA solution (0.05%/0.02% in calcium- and magnesium-free phosphate-buffered saline) and reseeded in 24-well plates (Nunc, Roskilde, Denmark) at a concentration of (7.5−10) × 10^3 cells/well or in six-well plates at a concentration of (25−30) × 10^4 cells/well and grown to 80% confluence.

Primary Bronchial Epithelial Cells. The establishment of the PBEC is described in detail in previous publications.[57,58] The cells were cultured in 80 cm^2 plastic flasks (Nunc, Roskilde, Denmark) at a density of (1−2) × 10^6 in keratinocyte serum-free medium (Gibco), supplemented with epidermal growth factor (5 ng/mL; Gibco), bovine pituitary extract (50 μg/mL; Gibco), and penicillin/streptomycin. The cultures were kept at 37 °C in a humidified atmosphere of 5% CO_2 in air, and medium was changed every second day. At confluence the cells were detached by exposure to trypsin/EDTA solution (0.03%/0.01% in calcium- and magnesium-free phosphate-buffered saline, PBS) and reseeded in 24-well plates (Nunc, Roskilde, Denmark) at a concentration of (7.5−10) × 10^3 cells/well or in six-well plates at a concentration of (25−30) × 10^4 cells/well and grown to 80% confluence.

Particle Exposure. Primary bronchial epithelial cells and A549 cells were incubated in media alone as control or Pd-NP at a concentration of 0.01−10 μg/mL for 24 h. Cells were also stimulated with TNF-α (1 ng/mL; R&D Systems, Europe, Abingdon, UK) alone or in combination with Pd-NP (0.01 or 10 μg/mL). As a positive control TNF-α at a concentration of 10 ng/mL was used. The A549 cells were also incubated with Al_2O_3 alone or $PdAl_2O_3$ at a concentration of 25−75 μg/mL for 24 h. After incubation, the supernatants were collected and centrifuged at 1000*g* for 10 min to remove cell debris and stored at −70 °C until analysis. Each experiment was performed three to five times in triplicates, with the exception of the combined exposure of Pd-NP (0.01 μg/mL) and TNF-α (1 ng/mL) and the Al_2O_3 experiments, which were performed twice in triplicate.

Cytotoxicity Assays. *Vital Dye Exclusion.* Cell viability was assessed using Trypan blue (0.4% in saline; Sera-Lab, Sussex, UK) as described previously.[59] Cells were examined by light microscopy, and the percentage of viable and dead cells was calculated.

Hypodiploid DNA Content. Cells were harvested and resuspended in a solution containing propidium iodide (50 μg/mL), 0.1% Triton X-100, and 0.1% sodium citrate in PBS as described.[60] Cells were analyzed on a FACScan (Becton−Dickinson, San Jose, CA, USA) equipped with a 488 nm argon laser using the CellQuest software (Becton−Dickinson). Data are presented as the percentage of cells displaying hypodiploid (sub-G1) DNA content.

DEVD-AMC Cleavage. Cleavage of the fluorogenic substrate DEVD-AMC, indicative of caspase-3-like enzyme activity, was determined as previously described.[61] Briefly, cell lysates and substrate (50 μM) were combined in a standard reaction buffer (100 mM Hepes, 10% sucrose, 5 mM dithiothreitol, and 0.1% CHAPS; pH 7.25) and added to a 96-well plate. Enzyme-catalyzed release of AMC was measured at 37 °C with a kinetic cycle of 26 time points using a TECAN Infinite 200 plate reader (Tecan Group Ltd., Männedorf, Switzerland) at excitation wavelength 380 nm and emission wavelength 460 nm. Fluorescence units were converted to picomoles of AMC using a standard curve generated with free AMC.

Western Blotting. Cells were lysed on ice for 30 min in RIPA buffer (50 mM Tris, pH 8.0, 150 mM NaCl, 10% glycerol, 1% NP-40, 0.5% deoxycholate) supplemented with protease inhibitors (Roche Diagnostics, Mannheim, Germany). Supernatant was retrieved after centrifugation of the cell lysates at 13 000 rpm. Equal amounts of protein (50 μg) were resolved by electrophoresis on a 4−12% SDS−polyacrylamide gel (Invitrogen, Carlsbad, CA, USA) and transferred to polyvinylidene difluoride membranes (Bio-Rad Laboratories, Hercules, CA, USA). The membranes were incubated with blocking buffer containing 0.1% Tween-20 and 5% milk and probed with rabbit polyclonal antiactive caspase-3 antibody (Sigma-Aldrich, St. Louis, MO, USA). Following incubation with horseradish peroxidase-conjugated anti-rabbit secondary antibodies (DAKO, Glostrup, Denmark), bound antibody was visualized with enhanced chemiluminescence (Thermo Scientific, Rockford, IL, USA).

DHE Assay. Production of superoxide was assessed by oxidation of dihydroethidium (DHE) to ethidium. Cells exposed or not exposed to Pd-NPs were incubated with 5 μM DHE (Molecular Probes, Eugene, OR, USA) in the relevant tissue culture medium for 40 min at 37 °C and then harvested,

resuspended in PBS, and submitted to flow cytometric analysis using a FACScan flow cytometer (Becton–Dickinson) operating with CellQuest software.

Assessment of Biomarkers. Interleukin-8 was measured in supernatants with an ELISA developed in-house.[62] Commercially available antibody pairs MAB208 and BAF208 (R&D Systems, Europe) were used as previously described. The detection limit was 40–3200 pg/mL. Prostaglandin E_2 was measured with commercially available monoclonal EIA kit, and the detection limit was 15–1000 pg/mL (Cayman Chemical Company, Ann Arbor, MI, USA). For duplicate samples an intra-assay coefficient of variation of <10% was accepted. The IL-8 levels in cell-free culture media for both cell types alone or in combination with the Pd-NPs at 0.01 and 10 μg/mL or the solution media that the particles are dissolved in were all below detection limit. Regarding PGE_2 all these combination resulted in low and similar levels regardless of combination (15–35 pg/mL), which were close to the detection limit.

Uptake Studies. Both A549 cells and PBEC were incubated with Pd-NP (10 μg/mL) for 2 h and fixed in 2% glutaraldehyde in 0.1 M sodium cacodylate buffer containing 0.1 M sucrose and 3 mM $CaCl_2$, pH 7.4, for 10 min. Cells were gently scraped to detach from cell culture plastics, pelleted, and fixed for an additional 24 h in the fixation solution mentioned above. The pellets were then rinsed in 0.15 M sodium cacodylate buffer containing 3 mM $CaCl_2$, pH 7.4. Postfixation of pellets was carried out in 2% osmium tetroxide in 0.07 M sodium cacodylate buffer containing 1.5 mM $CaCl_2$, pH 7.4, at 4 °C for 2 h, dehydrated in ethanol followed by acetone, and embedded in LX-112 (Ladd, Burlington, VT, USA). Sections were contrasted with uranyl acetate followed by lead citrate and examined in a Tecnai 12 transmission electron microscope (Fei, The Netherlands) at 80 kV. Digital images were taken by a Veleta digital camera (Soft Imaging System, GmbH, Münster, Germany).

Acknowledgment. We are indebted to K. Hultenby at Clinical Research Center, Dept. of Laboratory Medicine, Karolinska Institutet, Karolinska University Hospital Huddinge, for the TEM characterization of biological samples and to R. Pazik at the Dept. of Chemistry, SLU, for experimental help and valuable discussions on solution synthesis and characterization of NPs. The authors would like to extend their gratitude to S. Hasan of Uppsala University and M. Ware of Nanosight Ltd for graciously providing instrumentation time for DLS and Nanosight measurements, respectively, and also to T. Nikkilä at the Dept. of Pathology, SLU, for expert assistance with TEM analysis. The authors express their gratitude to the Swedish Research Council FORMAS for support to the grant "Particle Impurities in Air: Express-Analysis and Health Effects" and the Seventh Framework Program of the European Commission (FP7-NANOMMUNE). The work was also supported by the Swedish MRC, Heart and Lung Foundation, Vinnova and Karolinska Institutet. M.K. is a postdoctoral fellow supported by the Osher Initiative for Research on Severe Asthma at Karolinska Institutet.

Supporting Information Available: X-ray powder diffraction data of Pd particles, TEM images for Pd and Pd–Al_2O_3 colloids, assessment of endotoxin contamination of Pd-NPs, and additional cytotoxicity data (Trypan blue exclusion and reactive oxygen species generation) as described in the main text. This material is available free of charge *via* the Internet at http://pubs.acs.org.

REFERENCES AND NOTES

1. Kaspar, J.; Fornasiero, P.; Hickey, N. Automotive Catalytic Converters: Current Status and Some Perspectives. *Catal. Today* **2003**, *77*, 419–449.
2. Fenger, J. Urban Air Quality. *Atmos. Environ.* **1999**, *33*, 4877–4900.
3. Zereini, F.; Alt, F. *Palladium Emissions in the Environment*; Springer: Germany, 2006; ISBN: 3-540-29219-5.
4. Gauderman, W. J.; Vora, H.; McConnell, R.; Berhane, K.; Gilliland, F.; Thomas, D.; Lurmann, F.; Avol, E.; Künzli, N.; Jerrett, M.; *et al.* Effect of Exposure to Traffic on Lung Development from 10 to 18 Years of Age: a Cohort Study. *Lancet* **2007**, *369*, 571–577.
5. Kampa, M.; Castanas, E. Human Health Effects of Air Pollution. *Environ. Pollut.* **2008**, *151*, 362–367.
6. Künzli, N.; Kaiser, R.; Medina, S.; Studnicka, M.; Chanel, O.; Filliger, P.; Herry, M.; Horak, F., Jr.; Puybonnieux-Texier, V.; Quénel, P.; *et al.* Public-Health Impact of Outdoor Traffic-Related Air Pollution: a European Assessment. *Lancet* **2000**, *356*, 795–801.
7. Rauch, S.; Hemond, H. F.; Peucker-Ehrenbrink, B.; Ek, K. H.; Morrison, G. M. Platinum Group Element Concentrations and Osmium Isotopic Composition in Urban Airborne Particles from Boston, Massachusetts. *Environ. Sci. Technol.* **2005**, *39*, 9464–9470.
8. Glaister, B. J.; Mudd, G. M. The Environmental Costs of Platinum-PGM Mining and Sustainability: Is the Glass Half-Full or Half-Empty? *Miner. Eng.* **2010**, *23*, 438–450.
9. Ravindra, K.; Bencs, L.; Van Grieken, R. Platinum Group Elements in the Environment and their Health Risk. *Sci. Total Environ.* **2004**, *318*, 1–43.
10. Rauch, S.; Hemond, H. F.; Barbante, C.; Owari, M.; Morrison, G. M.; Peucker-Ehrenbrink, B.; Wass, U. Importance of Automobile Exhaust Catalyst Emissions for the Deposition of Platinum, Palladium, and Rhodium in the Northern Hemisphere. *Environ. Sci. Technol.* **2005**, *39*, 8156–8162.
11. Goncalves, A.; Domínguez, J. R.; Alvarado, J. Determination of Pd, Pt and Rh in Vehicles Escape Fumes by GF-AAS and ICP-OES. *Talanta* **2008**, *75*, 523–527.
12. Limbeck, A.; Puls, C.; Handler, M. Platinum and Palladium Emissions from On-road Vehicles in the Kaisermühlen Tunnel (Vienna, Austria). *Environ. Sci. Technol.* **2007**, *41*, 4938–4945.
13. Winterstein, G.; Stahn, M.; Voigt, M.; Kühn, G. Ceramic Honeycomb Structures. *CFI Ceram. Forum Int.* **1998**, *75*, 8–16.
14. Acres, G. J. K.; Harrison, B. The Development of Catalysts for Emission Control from Motor Vehicles: Early Research at Johnson Matthey. *Top. Catal.* **2004**, *28*, 3–11.
15. Geiser, M.; Kreyling, W. G. Deposition and Biokinetics of Inhaled Nanoparticles. *Part. Fibre Toxicol.* **2010**, *7*, 2.
16. Oberdörster, G.; Oberdörster, E.; Oberdörster, J. Nanotoxicology: An Emerging Discipline Evolving from Studies of Ultrafine Particles. *Environ. Health Perspect.* **2005**, *113*, 823–839.
17. Warheit, D.; Webb, T. R.; Colvin, V. L.; Reed, K.; Sayes, C. M. Pulmonary Bioassay Studies with Nanoscale and Fine-quartz Particles in Rats: Toxicity is Not Dependant upon Particle Size but on Surface Characteristics. *Toxicol. Sci.* **2006**, *95*, 270–280.
18. Cheung, K. L.; Ntziachristos, L.; Tzamkiozis, T.; Schaurer, J. J.; Samaras, Z.; Moore, K. F.; Sioutas, C. Emissions of Particulate Trace Elements, Metals and Organic Species from Gasoline, Diesel, and Biodiesel Passenger Vehicles and their Relation to Oxidative Potential. *Aerosol Sci. Technol.* **2010**, *44*, 500–513.
19. Kalavrouziotis, I. K.; Koukoulakis, P. H. The Environmental Impact of the Platinum Group Elements (Pt, Pd, Rh) Emitted by the Automobile Catalyst Converters. *Water Air Soil Pollut.* **2009**, *196*, 393–402.
20. Colombo, C.; Monhemius, A. J.; Plant, J. A. Platinum, Palladium and Rhodium Release from Vehicle Exhaust Catalysts and Road Dust Exposed to Simulated Lung Fluids. *Ecotoxicol. Envrion. Safety* **2008**, *71*, 722–730.
21. Turner, A.; Price, S. Bioaccessibility of Platinum Group Elements in Automotive Catalytic Converter Particulates. *Environ. Sci. Technol.* **2008**, *42*, 9443–9448.
22. Kielhorn, J.; Melber, C.; Keller, D.; Mangelsdorf, I. Palladium – A Review of Exposure and Effects to Human Health. *Int. J. Hyg. Environ. Health* **2002**, *205*, 417–432.
23. Schmid, M.; Zimmermann, S.; Krug, H. F.; Sures, B. Influence of Platinum, Palladium and Rhodium as Compared with Cadmium, Nickel and Chromium on Cell Viability and Oxidative Stress in Human Bronchial Epithelial Cells. *Environ. Int.* **2007**, *33*, 385–390.
24. Speranza, A.; Leopold, K.; Maier, M.; Taddei, A. R.; Scoccianti, V. Pd-Nanoparticles Cause Increased Toxicity to Kiwifruit Pollen

Compared to Soluble Pd(II). *Environ. Pollut.* **2010**, *158*, 873–882.
25. Hayashi, Y.; Takizawa, H.; Inoue, M.; Niihara, K.; Suganuma, K. Ecodesigns and Applications for Noble Metal Nanoparticles by Ultrasound Process. *IEEE Trans. Electron Packag. Manuf.* **2005**, *28*, 338–343.
26. Lim, J.-S.; Kim, S.-Y.; Lee, S.-Y.; Stach, E. A.; Culver, J. N.; Harris, M. T. Biotemplated Aqueous-phase Palladium Crystallization in the Absence of External Reducing Agents. *Nano Lett.* **2010**, *10*, 3863–3867.
27. Kim, J.; Takahashi, M.; Shimizu, T.; Shirazawa, T.; Kajita, M.; Kanayama, A.; Miyamoto, Y. Effects of a Potent Antioxidant, Platinum Nanoparticle, on the Lifespan of *Caenorhabiditis elegans*. *Mech. Ageing Dev.* **2008**, *129*, 322–331.
28. Pacardo, D. B.; Sethi, M.; Jones, S. E.; Naik, R. R.; Knecht, M. R. Biomimetic Synthesis of Pd Nanocatalysts for the Stille Coupling Reaction. *ACS Nano* **2009**, *3*, 1288–1296.
29. Li, H.; Jo, J. K.; Zhang, L. D.; Ha, C.-S.; Suh, H.; Kim, I. Hyperbranched Polyglycidol Assisted Green Synthetic Protocols for the Preparation of Multifunctional Metal Nanoparticles. *Langmuir* **2010**, *26*, 18442–18453.
30. Ornelas, C.; Aranzaes, J. R.; Salmon, L.; Astruc, D. "Click" Dendrimers: Synthesis, Redox Sensing of $Pd(OAc)_2$ and Remarkable Catalytic Hydrogenation Activity of Precise Pd Nanoparticles Stabilized by 1,2,3-Triazole-Containing Dendrimers. *Chem.—Eur. J.* **2008**, *14*, 50–64.
31. Kim, S. C.; Shim, W. G.; Rye, J. Y. Effect of the Growth of Nano-sized Pd Particle in 1 wt% Pd/-Al_2O_3 Catalyst on the Complete Oxidation of Volatile Organic Compounds. *Nanosci. Nanotechnol.* **2010**, *10*, 3521–3524.
32. Turova, N. Y.; Kessler, V. G.; Kucheiko, S. I. Molybdenum and Tungsten(VI) Bimetallic Alkoxides. Decomposition Accompanied by Dialkylether Elimination. *Polyhedron* **1991**, *10*, 2617–2628.
33. Kessler, V. G.; Shevelkov, A. V.; Bengtsson-Kloo, L. A. $MoO(O^iPr)_4$ Decomposition Pathways on Ageing: Spontaneous and Nearly Quantitative Transformation Into $Mo_6O_{10}(O^iPr)_{12}$ *Polyhedron* **1998**, *17*, 965–968.
34. Pazik, R.; Tekourite, R.; Håkansson, S.; Wiglusz, R.; Strek, W.; Seisenbaeva, G. A.; Yurii, K. G.; Kessler, V. Precursor and Solvent Effects in the Nonhydrolytic Synthesis of Complex Oxide Nanoparticles for Bioimaging Applications by the Ether Elimination (Bradley) Reaction. *Chem.—Eur. J.* **2009**, *15*, 6820–6826.
35. Kessler, V. G.; Nikitin, K. V.; Belokon, A. I. A New Argument in Favor of the Ether Elimination Mechanism: Formation of Acetals on Actions of Molybdenum Alkoxides on Carbonyl Compounds. *Polyhedron* **1998**, *17*, 2309–2311.
36. Seagrave, J.; Dunaway, S.; McDonald, J. D.; Mauderly, J. L.; Hayden., P.; Stidley, C. Responses of differentiated primary human lung epithelial cells to exposure to diesel exhaust at an air-liquid interface. *Exp. Lung Res.* **2007**, *33*, 27–51.
37. Filipe, V.; Hawe, A.; Jiskoot, W. Critical Evaluation of Nanoparticle Tracking Analysis (NTA) by NanoSight for the Measurement of Nanoparticles and Protein Aggregates. *Pharm. Res.* **2010**, *27*, 796–810.
38. Islam, M. A. Amphoteric CdSe Nanocrystalline Quantum Dots. *Nanotechnology* 2008, *19*, DOI: 10.1088/0957-4484/19/25/255708.
39. Vallhov, H.; Qin, J.; Johansson, S. M.; Ahlborg, N.; Muhammed, M. A.; Scheynius, A.; Gabrielsson, S. The importance of an Endotoxin-Free Environment during the Production of Nanoparticles used in Medical Applications. *Nano Lett.* **2006**, *6*, 1682–1686.
40. Dobrovolskaia, M. A.; Neun, B. W.; Clogston, J. D.; Ding, H.; Ljubimova, J.; McNeil, S. E. Ambiguities in Applying Traditional Limulus Amebocyte Lysate Tests to Quantify Endotoxin in Nanoparticle Formulations. *Nanomedicine (London)* **2010**, *5*, 555–562.
41. Palmberg, L.; Larsson, B.-M.; Malmberg, P.; Larsson, K. Induction of IL-8 Production in Human Alveolar Macrophages and Human Bronchial Epithelial Cells *in Vitro* by Swine Dust. *Thorax* **1998**, *53*, 260–264.
42. von Scheele, I.; Larsson, K.; Palmberg, L. Budesonide Enhances Toll-like Receptor 2 Expression in Activated Bronchial Epithelial Cells. *Inhal. Toxicol.* **2010**, *22*, 493–499.
43. Lunov, O.; Syrovets, T.; Loos, C.; Beil, J.; Delacher, M.; Tron, K.; Nienhaus, G. U.; Musyanovych, A.; Mailänder, V.; Landfester, K.; *et al*. Differential Uptake of Functionalized Polystyrene Nanoparticles by Human Macrophages and a Monocytic Cell Line. *ACS Nano* **2011**, *5*, 1657–1669.
44. Xia, T.; Kovochich, M.; Brant, J.; Hotze, M.; Sempf, J.; Oberley, T.; Sioutas, C.; Yeh, J. I.; Wiesner, M. R.; Nel, A. E. Comparison of the Abilities of Ambient and Manufactured Nanoparticles to Induce Cellular Toxicity According to an Oxidative Stress Paradigm. *Nano Lett.* **2006**, *6*, 1794–1807.
45. Monteiller, C.; Tran, L.; MacNee, W.; Faux, S.; Jones, A.; Miller, B.; Donaldson, K. The Pro-Inflammatory Effects of Low-Toxicity Low-Solubility Particles, Nanoparticles and Fine Particles, on Epithelial Cells in Vitro: The Role of Surface Area. *Occup. Environ. Med.* **2007**, *64*, 609–615.
46. Boscolo, P.; Bellante, V.; Leopold, K.; Maier, M.; Di Giampaolo, L.; Antonucci, A.; Iavicoli, I.; Tobia, L.; Paoletti, A.; Montalti, M.; *et al*. Effects of Palladium Nanoparticles on the Cytokine Release from Peripheral Blood Mononuclear Cells of Nonatopic Women. *J. Biol. Regul. Homeost. Agents* **2010**, *24*, 207–214.
47. Kajita, M.; Hikosaka, K.; Iitsuka, M.; Kanayama, A.; Toshima, N.; Miyamoto, Y. Platinum Nanoparticle is a Useful Scavenger of Superoxide Anion and Hydrogen Peroxide. *Free Radical Res.* **2007**, *41*, 615–626.
48. Hikosaka, K.; Kim, J.; Kajita, M.; Kanayama, A.; Miyamoto, Y. Platinum Nanoparticles have an Activity Similar to Mitochondrial NADH: Ubiquinone Oxidoreductase. *Colloid Surf. B* **2008**, *66*, 195–200.
49. Unfried, K.; Albrecht, C.; Klotz, L. O.; von Mikecz, A.; Grether-Beck, S.; Schins, R. P. F. Cellular Responses to Nanoparticles: Target Structures and Mechanisms. *Nanotoxicology* **2007**, *1*, 1–20.
50. Kunzmann, A.; Andersson, B.; Thurnherr, T.; Krug, H.; Scheynius, A.; Fadeel, B. Toxicology of Engineered Nanomaterials: Focus on Biocompatibility, Biodistribution and Biodegradation. *Biochim. Biophys. Acta* **2011**, *1810*, 361–373.
51. Lynch, I.; Salvati, A.; Dawson, K. A. Protein-Nanoparticle Interactions. What Does the Cell See? *Nat. Nanotechnol.* **2009**, *4*, 546–547.
52. Xia, X. R.; Monteiro-Riviere, N. A.; Riviere, J. M. An Index Characterization of Nanomaterials in Biological Systems. *Nat. Nanotechnol.* **2010**, *5*, 671–675.
53. Sund, J.; Alenius, H.; Vippola, M.; Savolainen, K.; Puustinen, A. Proteomic Characterization of Engineered Nanomaterial-Protein Interactions in Relation to Surface Reactivity. *ACS Nano* **2011**, DOI: 10.1021/nn101492k.
54. Fadeel, B.; Garcia-Bennett, A. E. Better Safe than Sorry: Understanding the Toxicology Properties of Inorganic Nanoparticles Manufactured for Biomedical Applications. *Adv. Drug Delivery* **2010**, *62*, 362–374.
55. Pavord, I. D.; Tattersfield, A. E. Bronchoprotective Role for Endogenous Prostaglandin E_2. *Lancet* **1995**, *345*, 436–438.
56. Swedin, L.; Neimert-Andersson, T.; Hjoberg, J.; Jonasson, S.; van Hage, M.; Adner, M.; Ryrfeldt, Å.; Dahlén, S. E. Dissociation of Airway Inflammation and Hyperresponsiveness by Cyclooxygenase Inhibition in Allergen Challenged Mice. *Eur. Respir. J.* **2009**, *34*, 200–208.
57. Strandberg, K.; Palmberg, L.; Larsson, K. Effect of Formoterol and Salmeterol on IL-6 and IL-8 Release in Airway Epithelial Cells. *Respir. Med.* **2007**, *101*, 1132–1339.
58. van Wetering, S.; van der Linden, A. C.; van Sterkenburg, M. A.; de Boer, W. I.; Kuijpers, A. L.; Schalkwijk, J.; Hiemstra, P. S. Regulation of SLPI and Elafin Release from Bronchial Epithelial Cells by Neutrophil Defensins. *Am. J. Physiol. Lung Cell Mol. Physiol.* **2000**, *278*, L51–58.
59. Witasp, E.; Kupferschmidt, N.; Bengtsson, L.; Hultenby, K.; Smedman, C.; Paulie, S.; Garcia-Bennett, A.-E.; Fadeel, B. Efficient Internalization of Mesoporous Silica Particles of Different Sizes by Primary Human Macrophages without Impairment of Macrophage Clearance of Apoptotic or Antibody-Opsonized Target Cells. *Toxicol. Appl. Pharmacol.* **2009**, *239*, 306–319.
60. Witasp, E.; Gustafsson, A. C.; Cotgreave, I.; Lind, M; Fadeel, B. Vitamin D Fails to Prevent Serum Starvation- or Staurosporine-Induced Apoptosis in Human and Rat

Osteosarcoma-Derived Cell Lines. *Biochem. Biophys. Res. Commun.* **2005**, *330*, 891–897.
61. Sun, Y.; Orrenius, S.; Pervaiz, S.; Fadeel, B. Plasma Membrane Sequestration of Apoptotic Protease-Activating Factor-1 in Human B-Lymphoma Cells: A Novel Mechanism of Chemoresistance. *Blood* **2005**, *105*, 4070–4077.
62. Larsson, K.; Tornling, G.; Gavhed, D.; Muller-Suur, C.; Palmberg, L. Inhalation of Cold Air Increases the Number of Inflammatory Cells in the Healthy Subjects. *Eur. Respir. J.* **1998**, *12*, 825–830.